

Diurnal and interannual variations of canopy urban heat island (CUHI) effects over a mountain–valley city with a semi-arid climate



Jiesheng Xue^{a,1}, Lian Zong^{a,1}, Yuanjian Yang^{a,*}, Xueyan Bi^b, Yanhao Zhang^a, Minghang Zhao^a

^a Collaborative Innovation Centre on Forecast and Evaluation of Meteorological Disasters, School of Atmospheric Physics, Nanjing University of Information Science & Technology, Nanjing 210044, China

^b Guangzhou Institute of Tropical and Marine Meteorology, China Meteorological Administration, Guangzhou, 510080, China

ARTICLE INFO

Keywords:

Canopy urban heat island
Heat wave
Local climate zone
Mountain–valley wind circulation
Mountain–valley city

ABSTRACT

Taking Lanzhou (a typical mountain–valley city in Northwest China) as an example, the diurnal and interannual variation characteristics of the canopy urban heat island (CUHI) and its relationship with heat waves (HWs), local climate zones (LCZs), mountain–valley wind circulation and aerosol pollution were explored. Results showed that the peak CUHI intensity (CUHII) in Lanzhou occurred at nighttime, while the minimum appeared in the daytime. The interannual variation of the CUHI fluctuated greatly, showing an upward trend. The average CUHII in HW periods was 103.6% higher than that in non-heat wave (NHW) periods. Longer-lasting HWs amplified the CUHII, in turn stronger CUHII led to more frequent HWs. The spatial variation of CUHIs mainly varied with LCZ types. In addition, relative to NHW periods, the mountain–valley wind circulation was strengthened during HW periods, favoring an increase in CUHII. On the one hand, the increased urban wind speed contributed to the enhancement of vertical turbulent heat transfer during HW periods. On the other hand, the ventilation conditions were improved, resulting in the reduced aerosol concentration, the urban canopy received more shortwave radiation, and the heat storage increased during HW periods. Both of these situations were conducive to enhanced CUHII.

1. Introduction

The canopy urban heat island (CUHI) effect is one of the major issues caused by urbanization and industrialization (Chen et al., 2022; Oke, 1973; Rizwan et al., 2008). The large amount of heat generated by urban structures as they consume and re-radiate solar radiation, and by other anthropogenic heat sources, are the main causes of CUHIs (Rizwan et al., 2008; Chen et al., 2020; Shi et al., 2022; Yang et al., 2022). Moreover, CUHIs can further aggravate the risk of urban heat waves (HWs), which can be a serious threat to human health and productivity (Fouillet et al., 2006; Fung et al., 2006; Geirinhas et al., 2020; Grigorieva and Lukyanets, 2021; Tong et al., 2021; Yang et al., 2020a). Therefore, CUHIs and HWs have emerged as important dual thermal-environment problems faced by

* Corresponding author.

E-mail address: yyj1985@nuist.edu.cn (Y. Yang).

¹ These authors contributed equally to this work.

most cities (Huang and Wang, 2019; Mohammad Harmay et al., 2021; Nakai et al., 1999).

Global warming has become an undeniable fact. Based on the average temperature change in the next 20 years, the rise in global temperature is expected to reach or exceed 1.5 °C (IPCC, 2021). HWs are considered to be one of the major phenomena in the context of global climate change. Their occurrence, severity and duration are likely to increase in the near future (Meehl and Tebaldi, 2004; Perkins et al., 2012; Rajulapati et al., 2022). Besides, HWs may be more severe in urban areas owing to the warming effects of CUHIs (Ngarambe et al., 2020; Zong et al., 2021; Liu et al., 2022). For example, Tan et al. (2010) found that, during HW periods, Shanghai

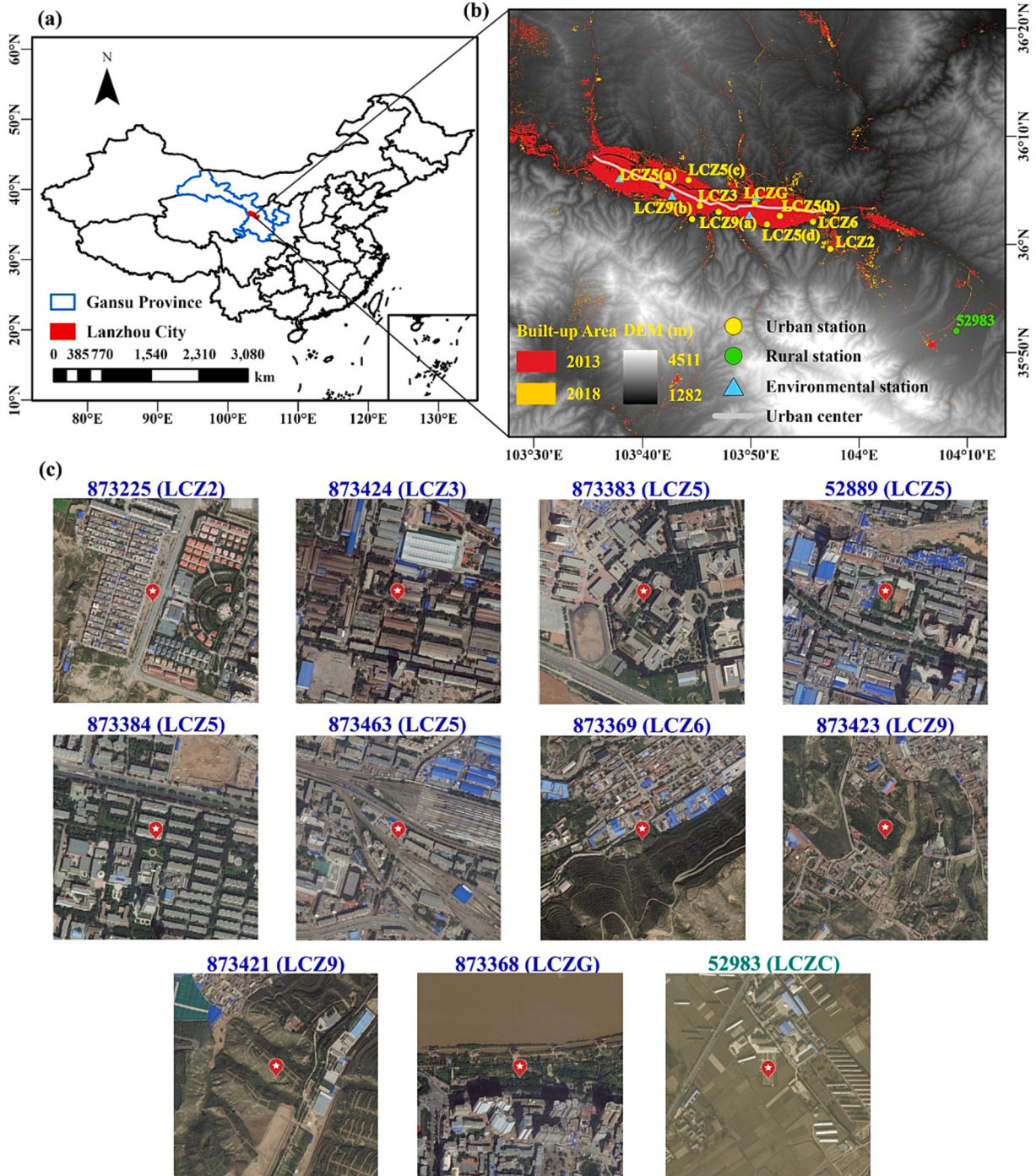


Fig. 1. (a) Map of China showing the location of the study area. (b) Geographical locations of the built-up area, surface weather stations and environmental monitoring stations. (c) Esri world images(700 m *700 m) of surface stations on 14 July 2017.

(China) had a higher degree of warming relative to surrounding areas, and Yang et al. (2019a) found that surface temperatures in 16 major metropolitan cities in the United States were 1.9 °C higher than their rural counterparts. Furthermore, heat-related mortality in urban areas during HW periods is higher than in rural areas (Grize et al., 2005; Rydman et al., 1999), which may be due to the synergistic effect of the interaction between CUHIs and HWs (Founda and Santamouris, 2017; Li and Bou-Zeid, 2013; Zong et al., 2021). Therefore, many countries have implemented intervention programs in metropolitan cities aimed at reducing the risks associated with urban high temperatures, such as in France (Fouillet et al., 2008), Milwaukee (USA) (Weisskopf et al., 2002) and Shanghai (Tan et al., 2006).

Previous studies have shown that there is significant positive feedback between CUHIs and HWs in some cities, such as Seoul, a coastal city with a temperate monsoon climate (Ngarambe et al., 2020); Beijing, an inland city located on a plain, with a warm temperate semi-humid and semiarid monsoon climate (Zong et al., 2021); and Athens, a coastal city with a Mediterranean climate (Founda and Santamouris, 2017). The enhancement of horizontal advective flux, as well as latent and sensible heat flux, are considered to be the primary causes of the obvious interactions between CUHIs and HWs in cities (Li and Bou-Zeid, 2013). However, CUHI–HW interaction is not obvious in some cities, such as Lisbon, a coastal city with a Mediterranean climate (Oliveira et al., 2021); Dijon, an inland city located on a plain, with a temperate marine climate (Richard et al., 2021); and Singapore, a coastal city with a tropical rainforest climate (Chew et al., 2021). For Seoul and Beijing (Ngarambe et al., 2020; Zong et al., 2021), it was found that the effects of their different local climate zones (LCZs) on CUHIs and HWs were also very different, because there may be differences in the convective flux and wind flow between different LCZ types (Li et al., 2021a; Zong et al., 2021). On the one hand, possibly attributable to the land-use characteristics of a given area, LCZs with a high density of buildings tend to exhibit strong differences in CUHI intensity (CUHII) between HW periods and non-heat wave (NHW) periods. On the other hand, it may be attributable to wind speed (WS). Higher WS is conducive to weakening the CUHI, and HWs generated by high-pressure anticyclones are often related to lower WS. Likewise, low WSs reduce horizontal advective cooling, leading to a strengthening of the CUHI.

Most previous studies have focused on coastal and inland-plain cities (e.g., Athens, Seoul, Beijing, Tokyo) (Founda and Santamouris, 2017; Mohammad Harmay and Choi, 2022; Ngarambe et al., 2020; Zong et al., 2021), with relatively little attention having been paid to CUHI–HW interaction in cities situated in valleys with a temperate continental semi-arid climate. Under clear-sky conditions, mountain–valley wind circulation can dominate the changes of local wind field and temperature field owing to the influence of terrain. In addition, mountain–valley wind circulation also affects the CUHI effect. Therefore, the changes in CUHIs in valley cities and their causes are a complex issue with many aspects needing clarification.

Therefore, taking Lanzhou in Northwest China as an example (a city located in a valley, surrounded by mountains, with rapid urbanization and a temperate continental semi-arid climate), observations from surface weather stations and environmental monitoring stations during 2013–2018 were used to study the synergistic effects of LCZs and WS on CUHIs and HWs, as well as the influences of local circulation and aerosol pollution.

2. Data and methods

2.1. Study area

The built-up area in Lanzhou increased from 4.48 km² in 1949 to 330.57 km² in 2019, and the population increased from about 86,000 in 1941 to about 3,790,900 permanent residents in the city by the end of 2019 (Li, 2021). The CUHI effect has increased gradually with the city's level of urbanization (Bai et al., 2005; Li et al., 2018), whose main urban area is situated in a river valley (width: 2–9 km; length: 40 km) (Fig. 1a). The terrain of the river valley being surrounded by two side mountains makes it easy for a thermal inversion layer to form, thus aggravating air pollution in the urban area. In addition, the meteorological conditions, i.e., light winds and stable stratification (especially inversion), can make it difficult for pollutants to disperse (Chu et al., 2008).

2.2. Data collection

Summertime hourly meteorological data (surface air temperature and WS) during 2013–2018, for ten urban sites and one rural site,

Table 1
LCZ types and temperature corrections for different weather stations.

Station	Lon. (°E)	Lat. (°N)	Elevation	Type	LCZ	Temperature correction (0.55 °C/100 m)
873,225	103.9558	35.9931	1587	Urban	LCZ2	0.38
873,424	103.7547	36.0594	1697	Urban	LCZ3	0.99
873,383	103.6969	36.0900	1534	Urban	LCZ5(a)	0.09
52,889	103.8778	36.0439	1517	Urban	LCZ5(b)	0
873,384	103.7372	36.0992	1543	Urban	LCZ5(c)	0.14
873,463	103.8581	36.0308	1555	Urban	LCZ5(d)	0.21
873,369	103.9292	36.0350	1590	Urban	LCZ6	0.40
873,423	103.7836	36.0500	1594	Urban	LCZ9(a)	0.42
873,421	103.7428	36.0389	1635	Urban	LCZ9(b)	0.65
873,368	103.8394	36.0633	1518	Urban	LCZG	0.01
52,983	104.1500	35.8667	1874	Rural	LCZC	1.96

were retrieved from surface weather stations in Lanzhou (<http://data.cma.cn/en>). The sites are characterized by different LCZs (Fig. 1, Table 1), as defined by Stewart and Oke (2012) (Table S1, Table S2), and the data were used to explore how the LCZs modulated HWS and the CUHI. We mainly employed visual interpretation method to indicate LCZ type high-resolution satellite image within the diameter range of 400–1000 m from the center of the station. LCZ5(c), LCZ5(d), LCZ9(b) and LCZG only appeared in Section 3.3 due to lack of wind data. According to Stewart and Oke (2012), LCZ2 describes a compact area with midrise buildings; LCZ3, a compact area with low-rise buildings; LCZ5, an open area with midrise buildings; LCZ6, an open area with low-rise buildings; LCZ9, an area in a natural setting with small or medium-sized buildings; LCZC, a bush area; and LCZG, a water body area. The altitudinal differences between the stations were large because of the considerable variation in the topography of Lanzhou. Therefore, according to the vertical thermal gradient of 0.55 °C/100 m, the air temperature data from all stations were adjusted to the same altitude as the lowest urban station (1517 m) (Table 1).

2.3. Methods

There is currently no universally agreed definition of an HW because of the different climatic conditions in different regions. Generally, HWS differ in three respects: temperature metric, intensity (i.e., temperature threshold), and duration (Xu et al., 2016). In this study, an HW was defined as when the diurnal maximum temperature was ≥ 33 °C for three consecutive days or more, as described by the “hot weather grade standard of Gansu province” (Liu et al., 2014). If an urban station experienced HW on a certain day, it was recorded as a “station occurrence”. The statistics of HW were independent at each weather station, so HW events may exceed one station occurrence on a day. The station occurrence indicates that total number of HW events for all stations at statistical period.

The definition of CUHII used in this study was as follows:

$$\text{CUHII} = \frac{1}{n} \sum_{i=1}^n T_{\text{Urban},i} - T_{\text{Rural}}, \quad (1)$$

where i indicates the number of urban station, n is the total number of urban stations; $T_{\text{Urban},i}$ is the temperature of the urban stations, and T_{Rural} that of the rural station. This urban–rural temperature difference approach provided a simple and systematic way to quantify the CUHI, but the rural reference area needs to be chosen appropriately to avoid inaccurate CUHI estimates. The rural station employed in this study (namely, station 52,983) was selected following the method of Cheng et al. (2020). The station is located on relatively flat terrain, surrounded by a large area of farmland, with a less impervious surface than the urban sites. In addition, to compare the difference in CUHII during HW periods and NHW periods more intuitively, ΔCUHII and $\Delta\text{CUHII}_{\max}$ were used to quantify the difference as follows:

$$\Delta\text{CUHII} = T_{\text{HW}} - T_{\text{NHW}}, \quad (2)$$

$$\Delta\text{CUHII}_{\max} = T_{\text{HW}(\max)} - T_{\text{NHW}(\max)}, \quad (3)$$

where T_{HW} and T_{NHW} are the CUHII of the urban stations during HW and NHW periods, respectively; $T_{\text{HW}(\max)}$ and $T_{\text{NHW}(\max)}$ are the maximum CUHII during HW and NHW periods, respectively.

In addition, k -means clustering into three categories (low, medium, high) was performed on the diurnal-average WS of every urban station to explore the potential impact of WS on the CUHI and HWS. Analysis of variance (ANOVA) was performed to assess the differences in CUHII under different WSs and LCZ types, and the statistical significance was tested at the 0.001 level. Silhouette coefficient was used to evaluate the clustering results. The value range of the silhouette coefficient is $[-1, 1]$, the larger the coefficient, the better the clustering effect. Since the National Meteorological Station cancelled cloud amount observation after 2013, we only counted the relationship between CUHI and WS under sunny days in 2013 for comparison. Sunny conditions are determined as those with $\leq 20\%$ daily total cloud cover (Yang et al., 2020b).

The mountain–valley wind circulation was superimposed on the background wind field, but it was difficult to observe the local circulation when the background wind was strong. Therefore, the large-scale background wind field needed to be removed first to calculate the mountain–valley wind. The calculations in this study were made with reference to previous research on lake–land and mountain–valley winds (Cao et al., 2015; Zheng et al., 2018). First, the station winds at each hour were decomposed into their u and v components, which represented the east–west and north–south winds, respectively. Next, the averages of the u and v components for each hour from July to August in 2013–2018 were calculated to obtain the hourly summer averages (\bar{u} and \bar{v}) at 0000–2300 LST. Then, the averages of all hourly u and v components from July to August in 2013–2018 were calculated to obtain the diurnal averages, U and V . And finally, by subtracting U and V from \bar{u} and \bar{v} , respectively, the hourly anomaly values (u' and v') were obtained. The diurnal averages (i.e., U and V) can be regarded as the system wind or background wind, while the hourly summer averages (i.e., \bar{u} and \bar{v}) can be regarded as the actual wind. The local wind was obtained by subtracting the system wind from the actual wind. Note that urban station 83,225 (LCZ2) was excluded from the valley wind calculation because of its location in another valley and not in the main urban area.

3. Results

3.1. Interannual and diurnal variation characteristics of CUHII in Lanzhou

During the warm season (May–September), Fig. 2a shows that there was obvious interannual fluctuation of CUHII in Lanzhou. The maximum CUHII values were 1.51 °C and 1.48 °C, in 2015 and 2017 respectively, and the minimum value was 1.15 °C, in 2013. In terms of the monthly variation in CUHII, it tended to be largest in June, followed by July, and smallest in September, at 1.63 °C, 1.51 °C and 1.03 °C, respectively (Fig. 2b).

The CUHII in Lanzhou was high from night to early morning, and low in the daytime, during the warm season (Fig. 3). It showed a slight upward trend at 0000–0600 LST, reaching a diurnal maximum of 1.72 °C at 0600 LST. After sunrise, the CUHII decreased rapidly, reaching a minimum of 0.31 °C at 0900 LST. Then, it continued to rise to 1.56 °C at 1700 LST, before beginning to decline, with another short-term recovery at 1900–2100 LST (Fig. 3g). In addition, it was found that, in 2015 and 2017, which were the years with the strongest CUHII, a higher CUHII was always maintained after sunset.

3.2. Interaction between the CUHI and HWs

The number of HWs that occurred in the warm season (May–September) was counted, and it was found that their distribution had strong monthly differences (Fig. 4). A total of 376 HWs occurred in the six years of the study period, within which the least occurred in September, with only 3 station occurrences. The number of HWs in July was the largest, followed by August, with 243 and 81 station occurrences, respectively. 86.17% HWs occurred in July and August. Therefore, to further explore the potential impact of HWs on the CUHI, the data from July and August were studied.

Figure 5 shows the diurnal variation of CUHII during HW and NHW periods. Overall, the six-year average CUHII ranges for HW and NHW periods were 0.86–3.22 °C and 0.23–1.58 °C, respectively. The diurnal variation trend of CUHII in HW periods was similar to that in NHW periods, but the intensities were always much higher. The CUHII was amplified during HW periods, indicating a synergistic effect between the CUHI and HWs.

Furthermore, Fig. 6 shows the diurnal variation of ΔCUHII and $\Delta\text{CUHII}_{\text{max}}$, in which their curves are roughly consistent. Overall, ΔCUHII was roughly bimodal, with its average value ranging from 0.52 °C to 1.73 °C. At night, it continued to rise until a peak of 1.61 °C at 0600 LST, a minimum of 0.52 °C at 0800 LST, and then a maximum of 1.73 °C at 1600 LST. The consistently positive values of ΔCUHII indicate that the CUHII in HW periods was always larger than that in NHW periods, and the CUHII in HW periods was enhanced by 1.22 °C, which was 103.6% higher than that in NHW periods. The CUHI was amplified in HW periods, and this enhancement fed back positively to the HWs (Luo and Lau, 2018; Ngarambe et al., 2020; Zong et al., 2021)—a synergistic effect that also exhibited diurnal variation.

3.3. Effect of LCZs on CUHI and HWs

Among all the urban stations, the most HW events with 91 appeared at station 873,383 (LCZ5), more than the rural station by 600%. LCZG had the least HW events (only 14), still higher than the rural station by 7.7% (Fig. 7a). In contrast, only 13 HW events occurred in LCZC where the rural station was located. This suggests that urban areas always experience a higher exposure risk of HWs, and that the risk varies across urban areas. In addition, it was also found that there were large differences in CUHII values under different urban stations. The strongest CUHII appeared at station 873,383 (LCZ5), followed by 873,384 (LCZ5), at 2.26 °C and 1.90 °C, which higher than the averaged CUHII in urban areas by 68.7% and 41.8%, respectively; and the minimum CUHII was 0.01 °C for LCZ2 (Fig. 7b). Furthermore, CUHII and HWs of all stations were positively correlated. The correlation coefficient between CUHII and HWs is 0.7351, which passes the 0.05 significance level (Fig. 7c). This indicates that longer-lasting HWs amplified the CUHII, and a stronger

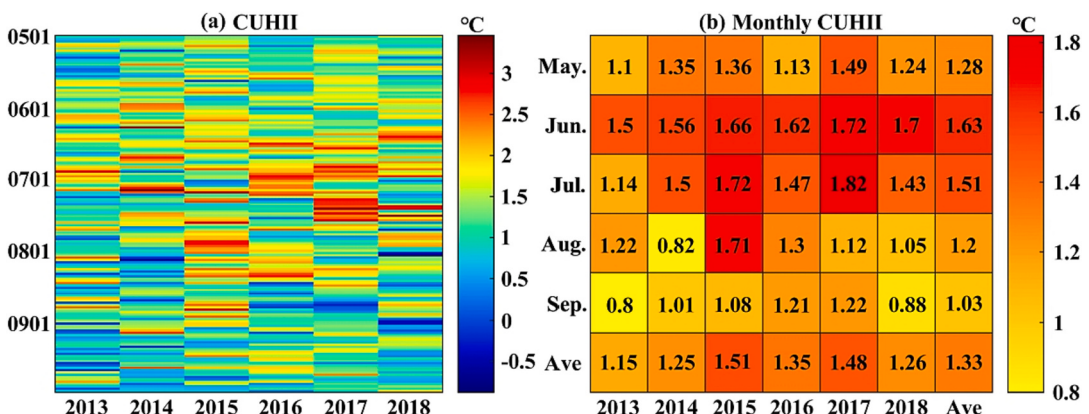


Fig. 2. CUHII in the warm season (May–September) of 2013–2018: (a) average diurnal CUHII; (b) average monthly CUHII.

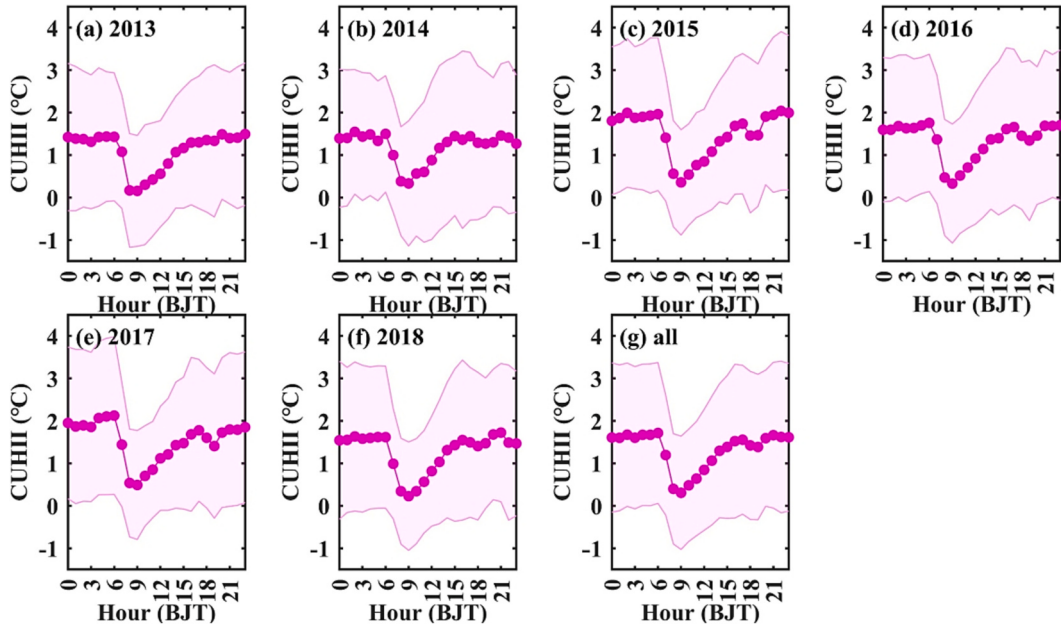


Fig. 3. Diurnal variation of CUHII in the warm season (May–September) of 2013–2018. Lines denote average CUHII values, and shaded areas denote the standard deviation of the average CUHII values according to all urban reference stations.

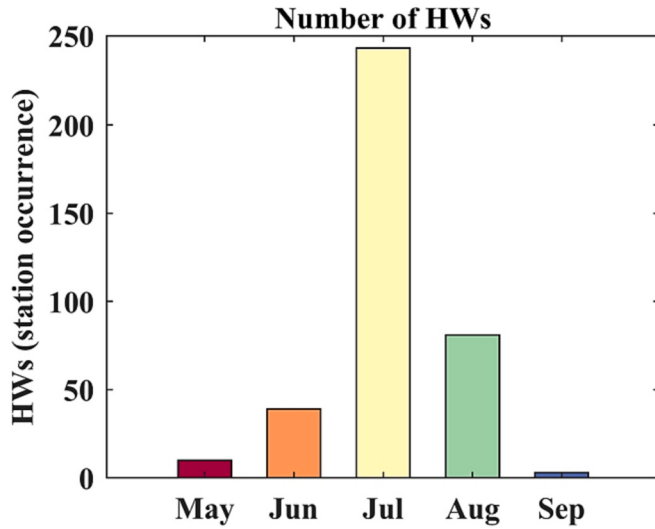


Fig. 4. Frequency of HWs in the warm season in summertime (May–September) during 2013–2018.

CUHII led to a higher frequency of HWs.

For the same LCZ type (e.g., LCZ 5), the farther away from the city center, the lower CUHII, showing intraclass difference (Fig. 7d). For different LCZs, the CUHII exhibited interclass difference. The CUHII of LCZ5 and LCZ6 with denser buildings were much stronger than LCZ9, indicating that lower building density with good ventilation can reduce CUHII. LCZG is located in the center of the city, but the CUHII was only 0.70 °C, which was lower than that at the edge of the city. This is because water body or bare/vegetation-covered soils increase evapotranspiration, resulting in a cooling effect (Li and Bou-Zeid, 2013; Chen et al., 2022). Despite the high density of buildings in LCZ2, its CUHII was significantly lower than those of the other LCZs, which may be because LCZ2's location is very far away from the city center and in another small valley outside the main urban area. In addition, note that the difference of CUHIs with LCZ2 and LCZ5 should also be attributed to the morphology difference between LCZ2 and LCZ5 (Li et al., 2020; Li et al., 2021b). This is because different building density can affect the surface albedo and emissivity and so on, further affect the radiation and turbulent flux and finally affect air temperature. Both the inter- and intra-class difference in CUHII indicate that there are obvious influence of density and morphology on the CUHII (Li et al., 2020; Zheng et al., 2022).

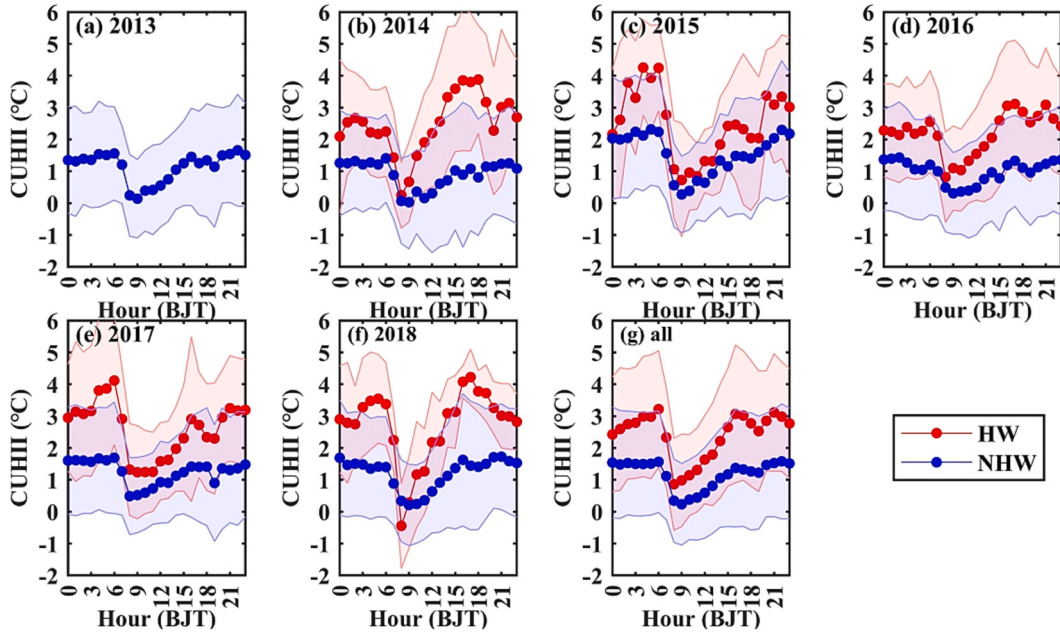


Fig. 5. Diurnal variation of CUHII during HW and NHW periods in the warm season (July–August) of 2013–2018. HW and NHW periods are indicated by red and blue, respectively. Lines denote average CUHII values, and shaded areas denote the standard deviation of the average CUHII values according to all urban reference stations. (For interpretation of the references to colour in this figure legend, the reader is referred to the web version of this article.)

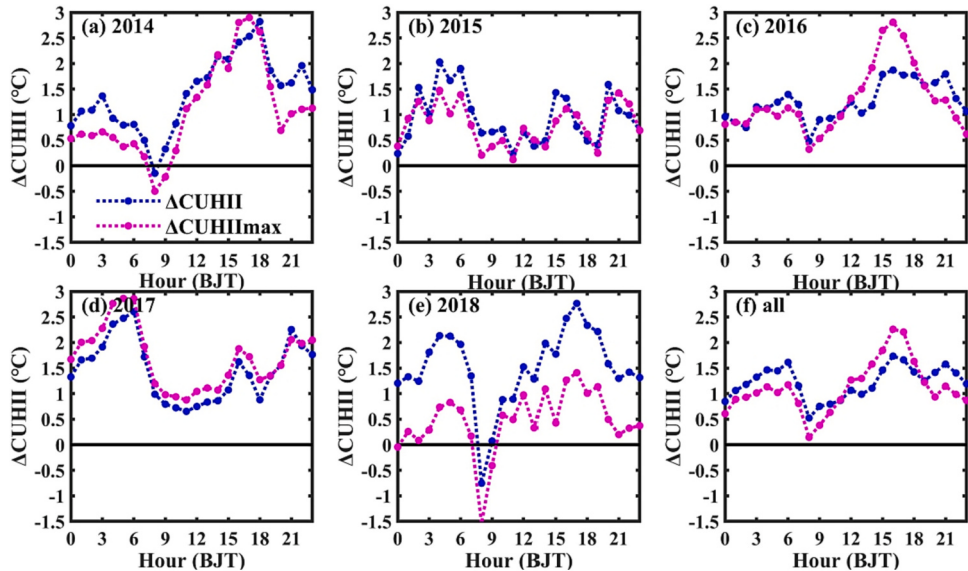


Fig. 6. Diurnal variation of ΔCUHII and $\Delta\text{CUHII}_{\text{max}}$ during HW and NHW periods in the summertime (July–August) of 2013–2018. Pink lines denote average $\Delta\text{CUHII}_{\text{max}}$ values, and blue lines denote average ΔCUHII values according to all urban reference stations. (For interpretation of the references to colour in this figure legend, the reader is referred to the web version of this article.)

3.4. Effect of WS on the CUHI and HWs

The k -means clustering technique was applied to the diurnal average of the WS data to assess the impact of WS on the HWs and CUHII. By selecting three clustering centers, the diurnal average WS could be divided into three categories: low, medium, and high WS (Fig. 8).

Each urban station experienced different frequencies of HWs under the three WS conditions (Fig. 9a, Fig. S1). A total of 57, 170 and

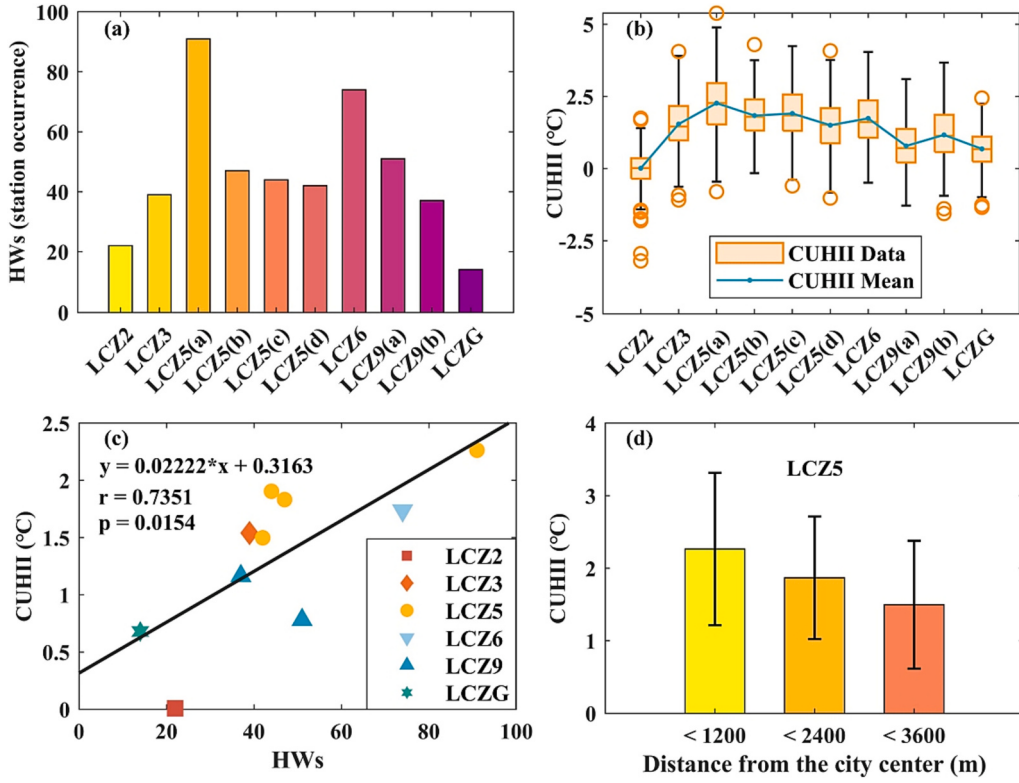


Fig. 7. Frequency of HWs (a), box plots of the average daily CUHII (b), scatter plots between HWs and CUHII (c) and CUHII of LCZ5 at different locations from the city center (d) in the summertime (July–August) of 2013–2018. For (b), the central box denotes the values from the lower to upper quartile (25th to 75th percentile). The vertical line extends from the maximum to the minimum value, and the circles denote outliers. The orange and green solid lines denote the median and the average values, respectively. For (d), the solid black lines denote the standard deviation. (For interpretation of the references to colour in this figure legend, the reader is referred to the web version of this article.)

97 HWs occurred under low, medium and high WS conditions, respectively. Proportionally, the number of HWs that occurred under the conditions of medium and high WS was much higher than that under low WS, exceeding 198.25% and 70.18% respectively. In addition, since the three WS groups contain different numbers of points during k-means clustering (Fig. 8), HWs was divided by the size of WS groups to eliminate the interference of different days under low, medium, and high WS conditions (Fig. 9b). Proportionally, the rates under the conditions of high and medium WS were much higher than that under low WS, exceeding 228.06% and 152.15%, respectively. Contrary to the previous found view, the WS in Lanzhou area was positively correlated with the frequency of HWs (Zong et al., 2021).

LCZ3 was also located on the edge of the main urban area, with a higher density of buildings and a smaller bare-soil area than LCZ6, but its CUHII was lower than that of LCZ6. This may have been because the altitude of the urban station corresponding to LCZ3 was 107 m higher than that of LCZ6. The wind in LCZ3 experienced less friction, so the WS was much faster than in the other LCZs, with LCZ3 having a mean WS that was 1.97 times that of LCZ6 (Fig. S2). Urban ventilation can reduce local warming, and this cooling effect of WS has been demonstrated in areas ranging from those with low-rise buildings to open areas with mid-rise buildings (He et al., 2020a, 2020b). It has also been shown in a previous study that the CUHII was close to zero above a certain WS threshold (He, 2018). Except for LCZ2 (for which the average CUHII value was negative under low WS), the CUHII values of all the LCZs were positive under the different WS conditions (Fig. 9c). The average diurnal CUHII values of the six urban stations were highest under high WS, followed by medium WS, and then lowest under low WS, at 1.88 °C, 1.51 °C and 0.91 °C respectively (Fig. S1d) under all weather conditions. Compared with the case under low WS, CUHII under high and medium WS conditions was enhanced by 107% and 66% (Fig. 9c). According to the ANOVA results between CUHII and WS, $F(2231) = 131.62$ and $p < 0.001$, meaning the difference in the average CUHII under the three WS categories was statistically significant. Besides, during sunny days (figures not shown), it was still found that CUHII was stronger under higher WS, e.g., the CUHII was 2.19 °C, 1.46 °C and 1.27 °C under high, medium and low WS condition respectively. In addition, the average WSs of all urban stations in HW and NHW periods were calculated, which were 1.22 m/s and 1.01 m/s, respectively. The average WS in HW periods was larger (~21%) than that in NHW periods.

It was found that Lanzhou had stronger WSs during HWs and strong CUHII periods, which is a complete contrast to the findings of previous studies for the temperate monsoon climate of Seoul (Ngarambe et al., 2020) and the warm temperate semi-humid and semiarid monsoon climate of Beijing (Zong et al., 2021). High WS conditions will weaken the CUHII (He, 2018), which is not conducive to the occurrence of HWs or a strong CUHII (Ngarambe et al., 2020; Zong et al., 2021). But why were WSs found to be higher in

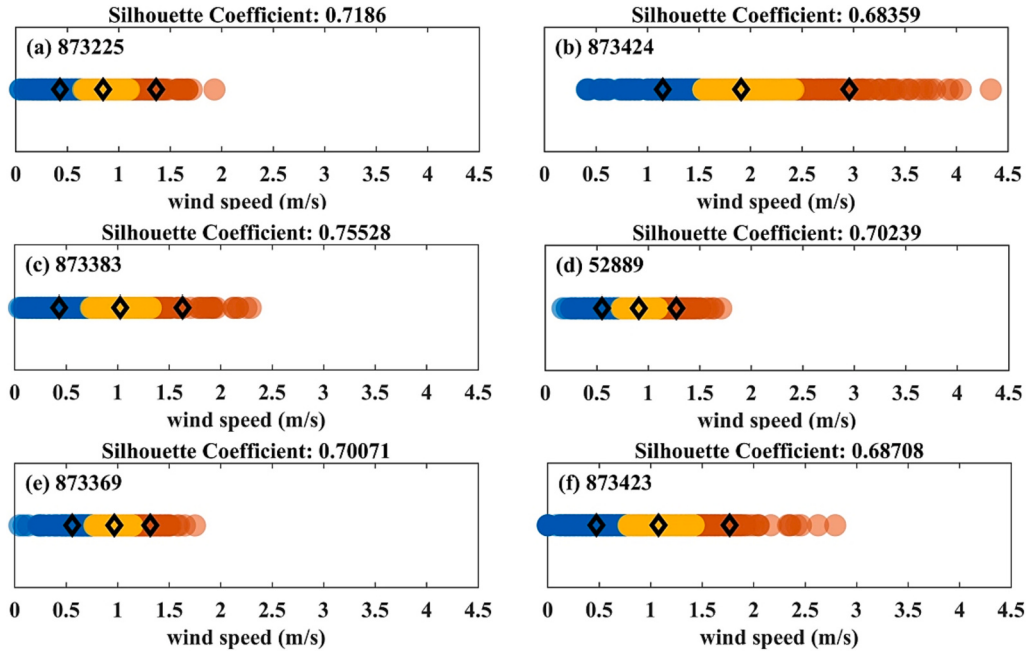


Fig. 8. K-means clustering results of average diurnal WSs in the summertime (July–August) from 2013 to 2018. The diamonds mark the cluster centers, and the titles are the silhouette coefficients. Due to the randomness of the k -means technique, the clustering results of the same urban station may be slightly different, so the clustering results with the silhouette coefficient closest to 1 were selected.

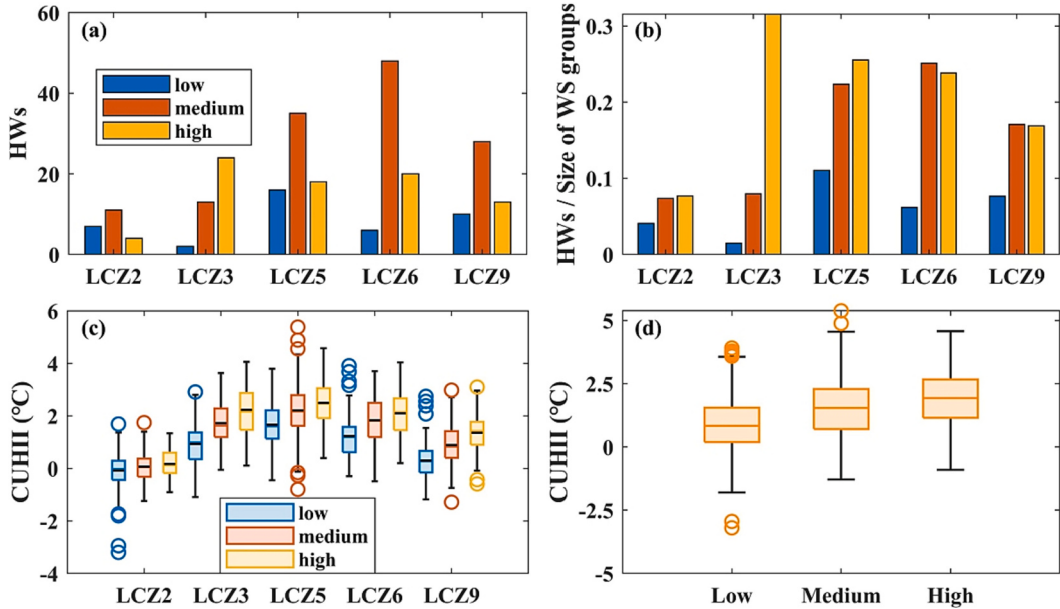


Fig. 9. Frequency of HWs (a), the value of HWs divided by size of WS groups (b), box plots of the average diurnal CUHII of different LCZs (c), and box plots of the average daily CUHII (d) under low, medium and high WS in the summertime (July–August) from 2013 to 2018. The central box denotes the values from the lower to upper quartile (25th to 75th percentile). The vertical line extends from the maximum to the minimum value, and the circles denote outliers. The solid lines of the same colors as the boxes denote the median value, and the middle black solid lines denote the average. (LCZ5 contains two urban stations, so the number of HWs and CUHII are the average of the two urban stations.)

Lanzhou during HWs and strong CUHII periods? This is discussed in the section 4.1.

In addition, Table 2 shows the two-way ANOVA results for the CUHII of different LCZs under different WS conditions. According to these results, $F(2231) = 6.43$ and $p < 0.001$, which was statistically significant. This is strong proof that the average CUHII differences

Table 2

Two-way ANOVA between LCZs and WS to CUHII.

Source	Sum Sq.	d.f.	Mean Sq.	F	Prob > F
LCZ	1005.81	4	251.453	398.88	4.74608e-259
WS	214.87	2	107.434	170.42	1.42289e-69
LCZ*WS	32.44	8	4.055	6.43	2.68887e-08
Error	1397.6	2217	0.63		
Total	2888.08	2231			

of the five LCZs types under the three WS conditions were statistically significant, and CUHII was more sensitive to the LCZ types.

Although it would be impractical to try to mitigate the synergistic effect of the CUHII and HWs by artificially affecting the WS over large areas, heat evacuation can be facilitated through long-term urban planning projects, such as the proper design of ventilation corridors (Yang et al., 2019b). Zheng et al. (2022) found that the construction of ventilation corridors in Beijing not only reduced the urban temperature and alleviated the CUHII, but also facilitated the diffusion of pollutants. In planning the construction of a city in a valley area, ventilation corridors should be devised by using the naturally generated mountain–valley wind circulation; and areas with a high density of high-rise buildings, where the risks from high temperatures will be greater, should be constructed in these ventilation corridors to improve urban health.

4. Discussion

4.1. Diurnal drivers of enhanced CUHII during HW periods

In section 3, enhanced CUHII was found during HW periods in Lanzhou, and the CUHI with HWs had a synergistic effect, which mirrored previous findings in some other large cities, such as Seoul (with a temperate monsoon climate) (Ngarambe et al., 2020), Beijing (with a warm temperate semi-humid and semiarid monsoon climate) (Zong et al., 2021), and Athens (with a Mediterranean climate) (Founda and Santamouris, 2017). However, Lanzhou also had higher WSs during HWs and strong CUHII periods, which was diametrically opposite to the findings related to the above three cities, in which the CUHII was found to decrease with an increase in WS; plus, the studies carried out in Seoul and Beijing found that WSs were lower during HW periods (Ngarambe et al., 2020; Zong et al., 2021). This suggests that there are terrain-specific physical mechanisms that drive the synergy between the CUHI and HWs in valley cities under a semi-arid climate. Valley cities have unique mountain–valley wind circulation, and they are not conducive to the diffusion of pollutants. Therefore, these two aspects are discussed to explore the driving factors of the valley wind circulation and aerosols for the enhancement of CUHII during HW periods.

4.1.1. Potential modulation of local mountain–valley circulation by HWs

During HW periods, the WS increased at almost all moments (Fig. 10a). The weather stations were all located in the southern part of the main urban area, so the valley wind circulation of these stations in summer was mainly regulated by the southern mountains. It can be seen from the Fig. 10b that the local wind circulation had obvious diurnal variations, with negative anomalies during the day (northeast wind) in the u and v directions, and positive anomalies (southwest wind) at night, which was due to the alternation of mountain–valley circulation (Zardi and Whiteman, 2013). The anomaly amplitudes of the local wind components in the u and v directions during HW periods were larger than those in NHW periods (Fig. 10b, Fig. S3), indicating that the local wind had a greater influence in HW periods. It is inferred, therefore, that the urban mountain–valley wind circulations are usually stronger in HW periods

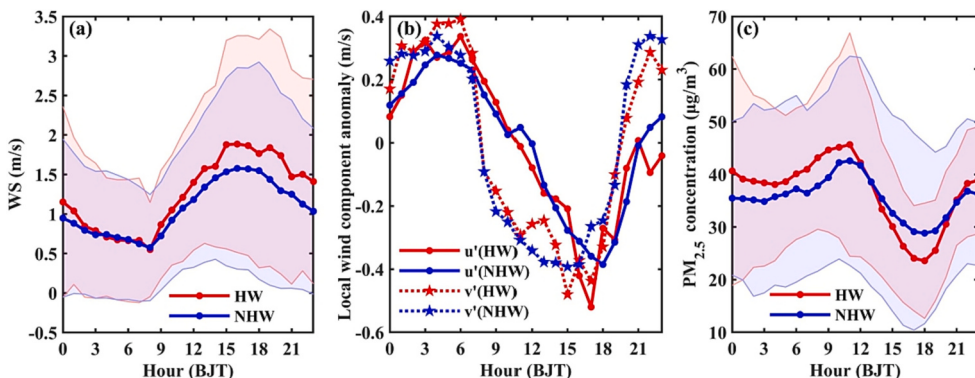


Fig. 10. Diurnal variation of WS (a) and the local wind component anomaly (b) in the summertime (July–August) of 2013–2018. Diurnal variation of PM_{2.5} concentration (c) in the summertime (July–August) of 2014–2018. HW and NHW periods are indicated by red and blue, respectively. Shaded areas denote the standard deviation. (For interpretation of the references to colour in this figure legend, the reader is referred to the web version of this article.)

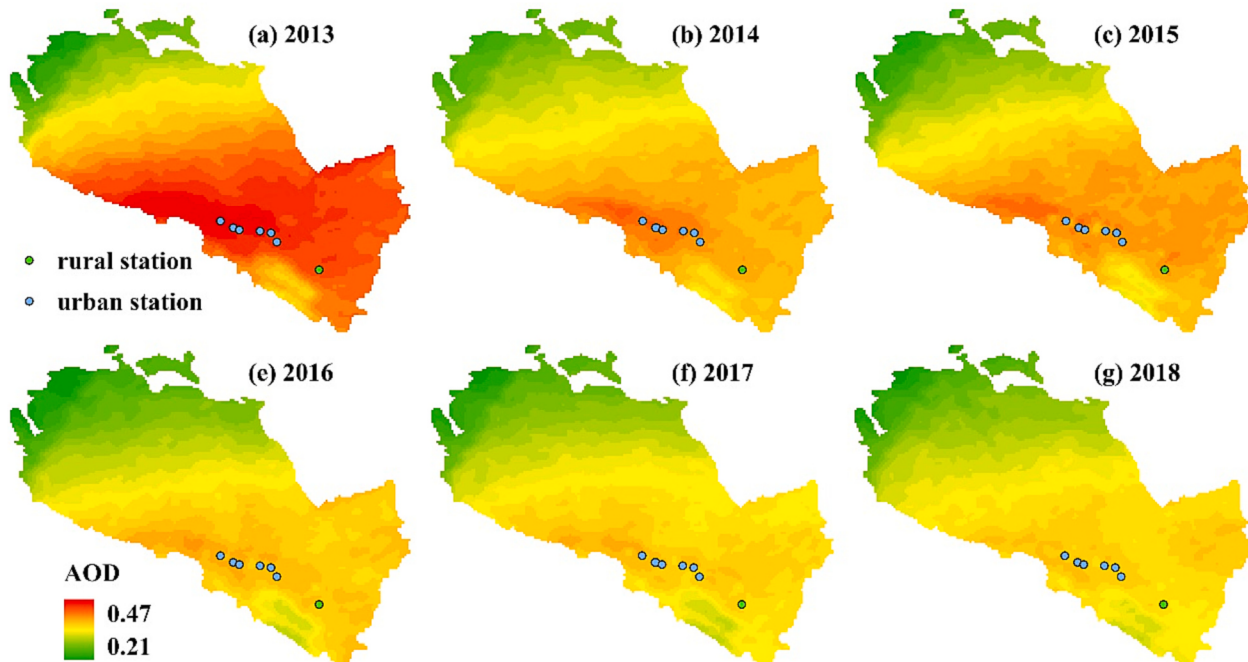


Fig. 11. Aerosol Optical Depth (AOD) of Lanzhou from 2013 to 2018.

than in NHW periods. The physical mechanism that may explain this phenomenon is as follows.

The generation of valley wind is due to the pressure gradient force driving the movement of air, and the pressure gradient is driven by both synoptic-scale and local temperature differences, which together act on hillsides and valley winds (Potter et al., 2018). HWs tend to have stronger solar radiation. Since there are more aerosols over the urban area than the hillsides in the north and south, the cooling (parasol) effect of aerosols absorbs and scatters solar radiation (Yang et al., 2020b), and the hillsides have larger heating areas, so they can obtain more radiation, thereby increasing the temperature difference between the northern and southern hillsides and the urban area. The increase in the local temperature difference may lead to an increase in the pressure gradient, thereby enhancing the daytime valley winds (Fig. 10b and c). For nighttime mountain wind, the urban surface can store more heat during the daytime of HW periods, and the surface radiates more longwave radiation to heat the atmosphere at night, which has a greater temperature difference with the rapidly cooling hillsides in the north and south after sunset, resulting in enhanced nighttime mountain wind (Fig. 10b). CUHII in HW periods was much higher than that in the NHW periods (Fig. 5), so the nighttime CUHII circulations were stronger, and the superposition with nighttime mountain winds resulted in enhanced mountain–valley wind circulation (Fig. 10b). This may explain why Lanzhou was accompanied by higher WSs during HW and strong CUHII periods.

4.1.2. Integrated modulation of mountain–valley circulation and aerosols

It was found that the warm-season mountain–valley wind circulation in Lanzhou can partly regulate the diurnal variation of aerosol concentration. As shown in Fig. 10c, the concentration of PM_{2.5} in Lanzhou increased from night to morning, and at the same time, mountain wind was conducive to blowing aerosols from mountain tops on the north and south sides back to the city. The PM_{2.5} concentration decreased from noon to afternoon, and the converted valley wind was conducive to blowing aerosols from the city to the mountain tops on the north and south sides. During HW periods, the PM_{2.5} concentration from night to morning was higher than that during NHW periods, which may have been partly due to the enhanced valley wind circulation, which was not conducive to the dispersion of pollutants. PM_{2.5} concentration in the afternoon was lower than that in NHW periods, which was also partly affected by the enhanced valley wind. This phenomenon further confirms the finding that the mountain–valley wind circulation is enhanced during HW periods.

For the overall CUHII (Fig. 3), the nighttime CUHII remained high and had a slight upward trend, which may be related to factors such as the negative surface radiation balance, inversion caused by the terrain, and aerosols. The density of the buildings on the urban underlying is high, and the “sky view factor” in the streets and courtyards is much smaller than that in the open spaces of rural areas. The heat of the longwave radiation from the surface is reflected multiple times between the walls and the ground, meaning the heat lost from the surface to the atmosphere is greatly reduced, resulting in slow cooling after sunset (Zhang et al., 2005). Related with the unique valley topography of Lanzhou, temperature inversion often occurs at night throughout the year, which is not conducive to the diffusion of heat at night. The impact of aerosols on the urban climate is mainly determined in two ways, direct and indirect effects, referred to as aerosol–radiation interactions and aerosol–cloud interactions, respectively (Yang et al., 2020b).

With the greater amount of aerosol pollution in the urban area (Fig. 11), more longwave radiation is emitted downward at night, compensating for the negative radiation balance at the surface and keeping the CUHII at a high level at night. After sunrise, with the gradual increase in the solar elevation angle, the rural area experiences a rapid increase in temperature owing to the small heat capacity of the soil, meaning the surface temperature difference begins to decrease and the CUHII decreases significantly. Coupled with the absorption and scattering of solar radiation by the severe aerosol pollution in the urban area in the early morning, urban warming is slower than in rural areas. Due to the absorption and storage of solar radiation by buildings, cement floors and concrete in the urban area, the heat capacity and thermal conductivity of the ground built with concrete are large, and thus the heat is stored during the day, meaning the CUHII begins to rise after reaching its minimum. In addition, the change of wind direction of mountain–valley wind is conducive to a reduction in aerosol concentration, which favors a lowering of the absorption and scattering of solar radiation by aerosols, which benefits the recovery of the CUHII. From 1900 LST to 2100 LST, the CUHII showed a slight upward trend, which may have been due to the heat generated by high levels of human activity, the mountain–valley wind had just started to change wind direction, and the mountain wind blew from the north and south hillsides to the valley bottom, which made the air adiabatically compressed and warmed.

In general, there is always an obvious difference in CUHII between HW and NHW periods, indicating that the CUHI and HWs have obvious positive feedback. The reason for this phenomenon may be because the increase in net heat flux in the urban area during HW periods is greater than that in rural areas (Zong et al., 2021). In Lanzhou, the enhanced mountain–valley wind circulation during HW periods will increase the WS, and this higher WS will weaken the CUHII (blue arrows in Fig. 12; He, 2018), which is not conducive to the occurrence of HWs and strong CUHII (Ngarambe et al., 2020; Zong et al., 2021). However, the increased surface WS contributes to the enhancement of vertical turbulent heat transport (red words in Fig. 12), which increases the surface heat flux. This then indirectly affects the air temperature and offsets the increased advection cooling (Li and Bou-Zeid, 2013). However, during HW periods, the enhanced mountain–valley wind circulation in the daytime is more conducive to a reduction in aerosol concentration, which reduces the absorption and scattering of solar radiation (blue arrows in Fig. 12). The urban canopy receives more shortwave radiation, and the increase in heat storage leads to an increase in CUHII (red words in Fig. 12). This indicates that the increase in surface heat flux and the decrease in aerosol concentration have a stronger effect on the increase in CUHII than that of the increase in WS on the mitigation of CUHII in the daytime (Fig. 12), resulting in enhanced CUHII during HW periods (Fig. 12).

At nighttime, the CUHII in HW periods is much larger than that in NHW periods, which may be due to the following reasons. On the one hand, the heat capacity of the urban underlying surface is larger than that of the rural area. During the day, more heat can be stored because of stronger solar radiation, and more longwave radiation is released at night. In addition, more man-made heat is added owing to the use of air conditioners. On the other hand, the nighttime aerosol concentration in HW periods is higher than that in NHW

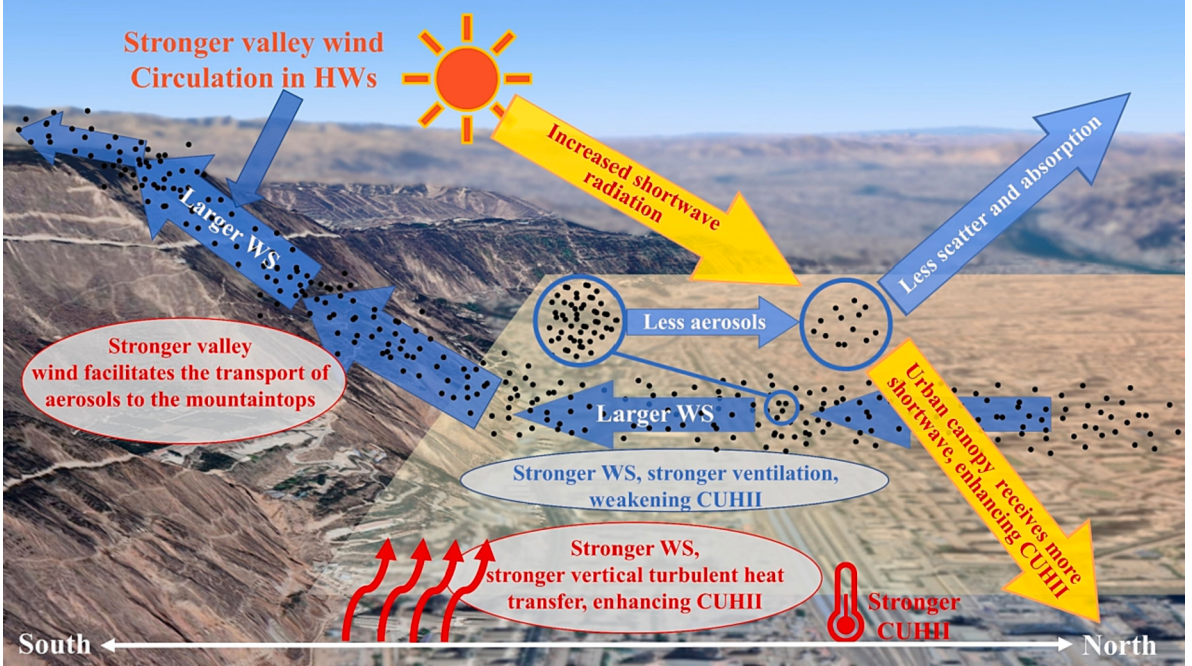


Fig. 12. Schematic of mechanisms of enhanced CUHI during HW events in the valley of Lanzhou city.

periods, and more longwave radiation is emitted downward to compensate for the negative radiation balance at the surface, and the frequent occurrence of temperature inversion at night is not conducive to heat diffusion.

In addition, the difference in CUHII between HW and NHW periods is usually small during 0800–0900 LST, and large at other times (Fig. 4) (i.e., Δ CUHII reaches its lowest values during 0800–0900 LST), which may also be partly related to changes in aerosol concentration due to enhancement of the valley wind circulation. The aerosol concentration after sunrise in HW periods is greater than that in NHW periods, and higher aerosol concentration will absorb and scatter more solar radiation, resulting in lower Δ CUHII.

4.2. Potential link between the interannual variability of HWs and CUHI

CUHII and HWs in Lanzhou have large interannual fluctuations. However, from the observations of the past six years employed in this study (2013–2018), it was found that, in July and August, when HWs occurred frequently, HWs (Fig. 13) and the CUHII (Fig. 2) had a good corresponding relationship in their interannual variation: periods of frequent HWs tended to have higher CUHII. For example, for the month of July, the year 2013 had the fewest HWs, and meanwhile the CUHII was the lowest in the six years; and the year 2017 had the most HWs, whilst at the same time the CUHII was at its largest. For the month of August, the years 2015 and 2016 had the most HWs and the largest CUHII. It seems that HWs have a moderating effect on the interannual variation of CUHII, for the long-term

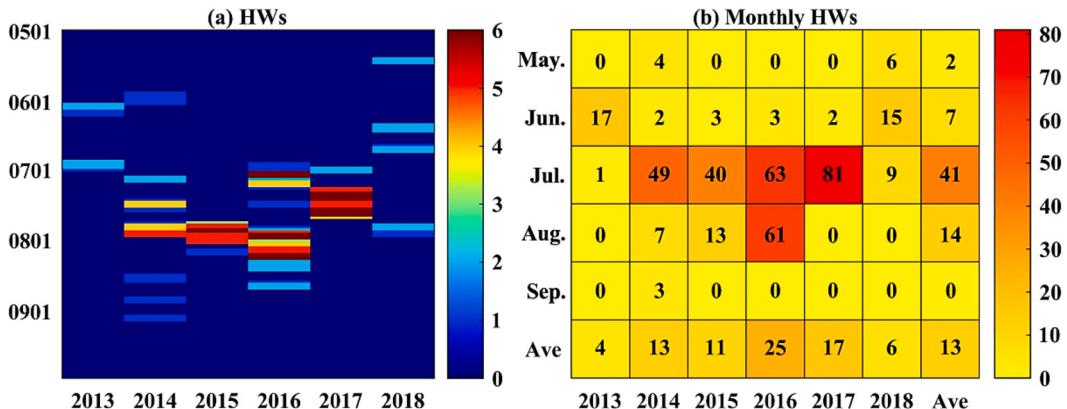


Fig. 13. Proportion of HWs in the summertime (May–September) of six urban stations during 2013–2018: (a) sum of diurnal HWs; (b) sum of monthly HWs. For (a), if a cell is bigger than 1, it means that more than one urban station experienced HW on that day.

variation trend of CUHII.

Analyzing the long-term series of HWs and CUHII in the past 63 years (1956–2018), it was found that the number of HWs and the CUHII in July and August had strong interannual changes, and both had an upward trend (Fig. 14). The upward trends of both HWs and the CUHII in July were faster than those in August, which further verifies the synergistic effect of the CUHI and HWs in the long-term series. Longer HWs led to enhanced CUHII, and stronger CUHII also increased the occurrence of HWs. The coefficient of determination (R^2) of HWs and CUHII in July and August in the 63-year time series was calculated and the result was $R^2 = 0.1955$, which indicates that HWs contribute as much as 19.55% to the interannual variation of the CUHI. In the context of global warming, the feedback of CUHI–HW interaction will further deteriorate, increasing the risk of extreme heat events in the urban area.

5. Conclusions

Based on observations from surface weather stations and environmental monitoring stations from 2013 to 2018, the diurnal and interannual variation characteristics of Lanzhou's CUHI and the effect of their associations with HWs, human factors (e.g., LCZs) and local background circulation factors (e.g., mountain–valley wind circulation) on the CUHI were explored. The main conclusions can be summarized as follows.

The CUHII was found to be stronger at night and weaker during the day. It drops sharply after sunrise, and even has an urban cold island effect, before then beginning to slowly rise in the afternoon. The change in CUHII during the day roughly presents a “V” shape. The interannual fluctuation of the CUHI is large, showing an overall upward trend.

Compared with NHW periods, the CUHII in HW periods increased by 1.22°C (around 103.6%), and the increase in CUHII had characteristics of diurnal variation, usually being more significant in the afternoon and early morning. There is positive feedback between the CUHI and HWs in Lanzhou; that is, longer HWs will amplify the CUHII, and a stronger CUHII will lead to a higher frequency of HWs. At the interannual scale, there is also positive feedback between the CUHI and HWs, and HWs contribute as much as 19.55% to the interannual variation of the CUHI.

The CUHII under different LCZs was significantly different, and was jointly determined by HWs, WS and the location of LCZs from the city center. Firstly, in LCZs that favor CUHII growth (e.g., areas with a high density of buildings), HWs may last longer, and longer HWs in turn increase the CUHII. Secondly, LCZs under strong WS have a cooling effect on the CUHII. For example, LCZ3 and LCZ6 were both located at the edge of the built-up area, and the buildings were denser in LCZ3, but the CUHII of LCZ3 was smaller than that of LCZ6. This slowed down the CUHII owing to the average WS of LCZ3 being 1.97 times that of LCZ6. Thirdly, the CUHII tended to be stronger in the LCZs closer to the city center.

In addition, it was further found that the mountain–valley wind circulation was enhanced during HW periods. On the one hand, the urban surface wind is accelerated, which helps to strengthen the vertical turbulent heat transport. On the other hand, ventilation conditions are improved, and aerosol concentrations are reduced, so more shortwave radiation is received by the urban canopy, and heat storage is increased. Both situations are conducive to the enhancement of the CUHII.

Overall, the mutual positive feedback effect of the CUHI and HWs exacerbates the risk of extreme HWs in cities. Under the dual influence of global warming and rapid urbanization, the mutual positive feedback effect of CUHIs and HWs will be further strengthened, and the threat to the health, lives and productivity of urban residents will be amplified. The current findings will serve as a useful reference for mountain–valley cities in other semi-arid regions of the world and provide scientific guidance for coping with

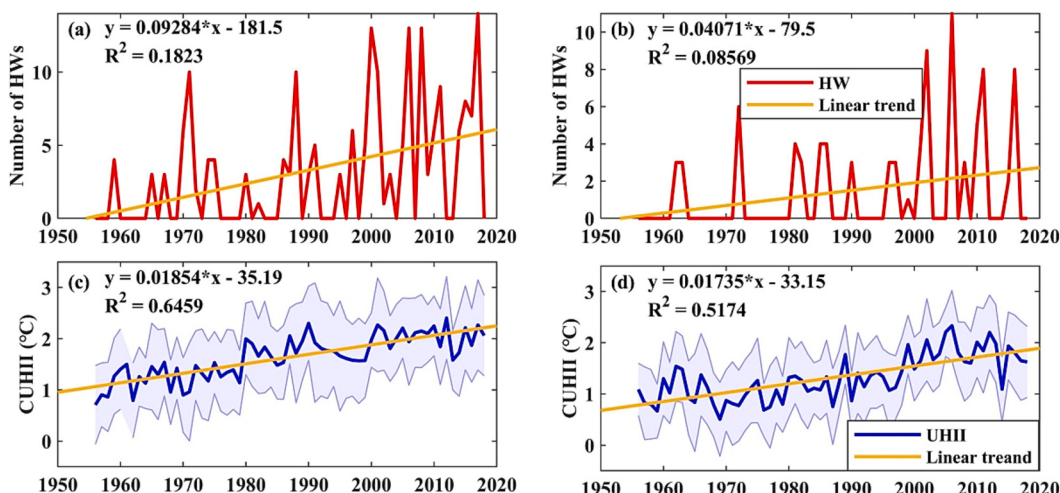


Fig. 14. HWs and the average CUHII in the past 63 summers (July–August) from 1956 to 2018: (a) HWs in July; (b) HWs in August; (c) average CUHII in July; (d) average CUHII in August. Shaded areas denote the standard deviation of the average CUHII, and yellow lines denote the linear trend of HWs and average CUHII. (The urban station is national station 52,889, and the rural station is national station 52,983). (For interpretation of the references to colour in this figure legend, the reader is referred to the web version of this article.)

various risks and hazards caused by extreme high temperatures in valley cities in warm season. In future research, state-of-the-art numerical simulation methods should be used to further reveal the fine-scale structure of mountain–valley wind circulation and the physical processes that affect the interaction and feedback of CUHIs and HWs.

Funding

This study was supported by the National Natural Science Foundation of China (grant no. 42222503 and 42175098).

Data availability statement

The DEM data were accessed at <http://www.tuxingis.com>, the built-up area data were accessed at <https://doi.org/10.1360/N072020-0370>, and the AOD data were accessed at <https://zenodo.org/record/5652257>.

CRediT authorship contribution statement

Jiesheng Xue: Methodology, Data curation, Formal analysis, Software, Visualization, Writing - original draft, Writing - review & editing. **Lian Zong:** Methodology, Formal analysis, Data curation, Investigation, Software, Validation, Writing - review & editing. **Yuanjian Yang:** Methodology, Formal analysis, Conceptualization, Funding acquisition, Supervision, Writing - review & editing. **Xueyan Bi:** Writing – review & editing. **Yanhao Zhang:** Visualization, Writing - review & editing. **Minghang Zhao:** Writing – review & editing.

Declaration of Competing Interest

The authors declare no conflict of interest.

Data availability

Data will be made available on request.

Acknowledgments

We acknowledge Experimental Teaching Center for Meteorology and Environment of NUIST for meteorological data and the High Performance Computing Center of Nanjing University of Information Science & Technology for their support of this work.

Appendix A. Supplementary data

Supplementary data to this article can be found online at <https://doi.org/10.1016/j.ulclim.2023.101425>.

References

- Bai, H., Ren, G., Fang, F., 2005. Characteristics of urban Heat Island effect and its influencing factors in Lanzhou. *Meteorol. Sci. Technol. Chin.* <https://doi.org/10.19517/j.1671-6345.2005.06.003>, 492–495+500.
- Cao, J., Liu, X., Li, G., Zou, H., 2015. Analysis of the phenomenon of Lake-land breeze in Poyang Lake area. *Plateau Meteorol. Chin.* 426–435.
- Chen, S., Yang, Y., Deng, F., Zhang, Y., Liu, D., Liu, C., Gao, Z., 2022. A high-resolution monitoring approach of canopy urban heat island using a random forest model and multi-platform observations. *Atmos. Meas. Tech.* 15, 735–756. <https://doi.org/10.5194/amt-15-735-2022>.
- Cheng, X., Lan, T., Mao, R., Gong, D., Han, H., Liu, X., 2020. Reducing air pollution increases the local diurnal temperature range: a case study of Lanzhou, China. *Meteorol. Appl.* 27 <https://doi.org/10.1002/met.1939>.
- Chew, L.W., Liu, X., Li, X.-X., Norford, L.K., 2021. Interaction between heat wave and urban heat island: a case study in a tropical coastal city, Singapore. *Atmos. Res.* 247, 105134 <https://doi.org/10.1016/j.atmosres.2020.105134>.
- Chu, P.C., Chen, Y., Lu, S., Li, Z., Lu, Y., 2008. Particulate air pollution in Lanzhou China. *Environ. Int.* 34, 698–713. <https://doi.org/10.1016/j.envint.2007.12.013>.
- Fouillet, A., Rey, G., Laurent, F., Pavillon, G., Bellec, S., Guihenneuc-Jouyaux, C., Clavel, J., Jouglard, E., Hémon, D., 2006. Excess mortality related to the august 2003 heat wave in France. *Int. Arch. Occup. Environ. Health* 80, 16–24. <https://doi.org/10.1007/s00420-006-0089-4>.
- Fouillet, A., Rey, G., Wagner, V., Laaidi, K., Empereur-Bissonnet, P., Le Tertre, A., Frayssinet, P., Bessemoulin, P., Laurent, F., De Crouy-Chanel, P., Jouglard, E., Hémon, D., 2008. Has the impact of heat waves on mortality changed in France since the European heat wave of summer 2003? A study of the 2006 heat wave. *Int. J. Epidemiol.* 37, 309–317. <https://doi.org/10.1093/ije/dym253>.
- Founda, D., Santamouris, M., 2017. Synergies between urban Heat Island and heat waves in Athens (Greece), during an extremely hot summer (2012). *Sci. Rep.* 7, 10973. <https://doi.org/10.1038/s41598-017-11407-6>.
- Fung, W.Y., Lam, K.S., Hung, W.T., Pang, S.W., Lee, Y.L., 2006. Impact of urban temperature on energy consumption of Hong Kong. *Energy* 31, 2623–2637. <https://doi.org/10.1016/j.energy.2005.12.009>.
- Geirinhas, J.L., Russo, A., Libonati, R., Trigo, R.M., Castro, L.C.O., Peres, L.F., Magalhães, M. de A.F.M., Nunes, B., 2020. Heat-related mortality at the beginning of the twenty-first century in Rio de Janeiro, Brazil. *Int. J. Biometeorol.* 64, 1319–1332. <https://doi.org/10.1007/s00484-020-01908-x>.
- Grigorieva, E., Lukyanets, A., 2021. Combined effect of hot weather and outdoor air pollution on respiratory health: literature review. *Atmosphere* 12, 790. <https://doi.org/10.3390/atmos12060790>.
- Grize, L., Huss, A., Thommen, O., Schindler, C., Braun-Fahrlander, C., 2005. Heat wave 2003 and mortality in Switzerland. *Swiss Med. Wkly.* 135, 200–205.

- He, B.-J., 2018. Potentials of meteorological characteristics and synoptic conditions to mitigate urban heat island effects. *Urban Clim.* 24, 26–33. <https://doi.org/10.1016/j.ulclim.2018.01.004>.
- He, B.-J., Ding, L., Prasad, D., 2020a. Urban ventilation and its potential for local warming mitigation: a field experiment in an open low-rise gridiron precinct. *Sustain. Cities Soc.* 55, 102028 <https://doi.org/10.1016/j.scs.2020.102028>.
- He, B.-J., Ding, L., Prasad, D., 2020b. Wind-sensitive urban planning and design: precinct ventilation performance and its potential for local warming mitigation in an open midrise gridiron precinct. *J. Build. Eng.* 29, 101145 <https://doi.org/10.1016/j.jobe.2019.101145>.
- Huang, X., Wang, Y., 2019. Investigating the effects of 3D urban morphology on the surface urban heat island effect in urban functional zones by using high-resolution remote sensing data: a case study of Wuhan, Central China. *ISPRS J. Photogramm. Remote Sens.* 152, 119–131. <https://doi.org/10.1016/j.isprsjprs.2019.04.010>.
- Li, D., Bou-Zeid, E., 2013. Synergistic interactions between urban Heat Islands and heat waves: the impact in cities is larger than the sum of its parts. *J. Appl. Meteorol. Climatol.* 52, 2051–2064. <https://doi.org/10.1175/JAMC-D-13-02.1>.
- Li, G., 2021. *Climate Effects of Valley-Type Cities: Pattern, Process, Mechanism and Regulation*, 1st ed. Science Press (in Chinese).
- Li, G., Zhang, X., Mirzaei, P.A., Zhang, J., Zhao, Z., 2018. Urban heat island effect of a typical valley city in China: responds to the global warming and rapid urbanization. *Sustain. Cities Soc.* 38, 736–745. <https://doi.org/10.1016/j.scs.2018.01.033>.
- Li, N., Yang, J., Qiao, Z., Wang, Y., Miao, S., 2021a. Urban thermal characteristics of local climate zones and their mitigation measures across cities in different climate zones of China. *Remote Sens.* 13 (8), 1468. <https://doi.org/10.3390/rs13081468>.
- Li, Y., Schubert, S., Kropp, J.P., Rybski, D., 2020. On the influence of density and morphology on the urban heat Island intensity. *Nat. Commun.* 11, 2647. <https://doi.org/10.1038/s41467-020-16461-9>.
- Li, Y., Zhou, B., Glockmann, M., Kropp, J.P., Rybski, D., 2021b. Context sensitivity of surface urban heat island at the local and regional scales. *Sustain. Cities Soc.* 74, 103146 <https://doi.org/10.1016/j.scs.2021.103146>.
- Liu, S., Yang, X., Chen, X., Yang, J., Zhou, G., 2014. Making standards for grade of hot weather in Gansu Province. *J. Arid Meteorol. Chin.* 659–664.
- Liu, X., Tian, G., Feng, J., Hou, H., Ma, B., 2022. Adaptation strategies for urban warming: assessing the impacts of heat waves on cooling capabilities in Chongqing, China. *Urban Clim.* 45, 101269 <https://doi.org/10.1016/j.ulclim.2022.101269>.
- Luo, M., Lau, N., 2018. Increasing heat stress in urban areas of eastern China: acceleration by urbanization. *Geophys. Res. Lett.* 45 <https://doi.org/10.1029/2018GL080306>.
- Meehl, G.A., Tebaldi, C., 2004. More intense, more frequent, and longer lasting heat waves in the 21st century. *Science* 305, 994–997. <https://doi.org/10.1126/science.1098704>.
- Mohammad Harmay, N.S., Choi, M., 2022. Effects of heat waves on urban warming across different urban morphologies and climate zones. *Build. Environ.* 209, 108677 <https://doi.org/10.1016/j.buildenv.2021.108677>.
- Mohammad Harmay, N.S., Kim, D., Choi, M., 2021. Urban Heat Island associated with land use/land cover and climate variations in Melbourne, Australia. *Sustain. Cities Soc.* 69, 102861 <https://doi.org/10.1016/j.scs.2021.102861>.
- Nakai, S., Itoh, T., Morimoto, T., 1999. Deaths from heat-stroke in Japan 1968–1994. *Int. J. Biometeorol.* 43, 0124. <https://doi.org/10.1007/s004840050127>.
- Ngarambe, J., Nganyiyimana, J., Kim, I., Santamouris, M., Yun, G.Y., 2020. Synergies between urban heat island and heat waves in Seoul: the role of wind speed and land use characteristics. *PLoS One* 15, e0243571. <https://doi.org/10.1371/journal.pone.0243571>.
- Oke, T.R., 1973. City size and the urban heat island. *Atmos. Environ.* 1967 (7), 769–779. [https://doi.org/10.1016/0004-6981\(73\)90140-6](https://doi.org/10.1016/0004-6981(73)90140-6).
- Oliveira, A., Lopes, A., Correia, E., Niza, S., Soares, A., 2021. Heatwaves and summer urban heat Islands: a daily cycle approach to unveil the urban thermal signal changes in Lisbon, Portugal. *Atmosphere* 12, 292. <https://doi.org/10.3390/atmos12030292>.
- Perkins, S.E., Alexander, L.V., Nairn, J.R., 2012. Increasing frequency, intensity and duration of observed global heatwaves and warm spells. *Geophys. Res. Lett.* 39 <https://doi.org/10.1029/2012GL053361>.
- Potter, E.R., Orr, A., Willis, I.C., Bannister, D., Salerno, F., 2018. Dynamical drivers of the local wind regime in a Himalayan Valley. *J. Geophys. Res.-Atmos.* 123 <https://doi.org/10.1029/2018JD029427>.
- Rajulapati, C.R., Gaddam, R.K., Nerantzaki, S.D., Papalexou, S.M., Cannon, A.J., Clark, M.P., 2022. Exacerbated heat in large Canadian cities. *Urban Clim.* 42, 101097 <https://doi.org/10.1016/j.ulclim.2022.101097>.
- Richard, Y., Pohl, B., Rega, M., Pergaud, J., Thevenin, T., Emery, J., Dudek, J., Vairet, T., Zito, S., Chateau-Smith, C., 2021. Is urban Heat Island intensity higher during hot spells and heat waves (Dijon, France, 2014–2019)? *Urban Clim.* 35, 100747 <https://doi.org/10.1016/j.ulclim.2020.100747>.
- Rizwan, A.M., Dennis, L.Y.C., Liu, C., 2008. A review on the generation, determination and mitigation of urban Heat Island. *J. Environ. Sci.* 20, 120–128. [https://doi.org/10.1016/S1001-0742\(08\)60019-4](https://doi.org/10.1016/S1001-0742(08)60019-4).
- Rydman, R.J., Rumoro, D.P., Silva, J.C., Hogan, T.M., Kampe, L.M., 1999. The rate and risk of heat-related illness in hospital emergency departments during the 1995 Chicago heat disaster. *J. Med. Syst.* 23, 41–56. <https://doi.org/10.1023/A:1020871528086>.
- Shi, T., Yang, Y., Sun, D., Huang, Y., Shi, C., 2022. Influence of changes in meteorological observational environment on urbanization Bias in surface air temperature: a review. *Front. Clim.* 3, 781999 <https://doi.org/10.3389/fclim.2021.781999>.
- Stewart, I.D., Oke, T.R., 2012. Local climate zones for urban temperature studies. *Bull. Am. Meteorol. Soc.* 93, 1879–1900. <https://doi.org/10.1175/BAMS-D-11-00019.1>.
- Tan, J., Zheng, Y., Song, G., Kalkstein, L.S., Kalkstein, A.J., Tang, X., 2006. Heat wave impacts on mortality in Shanghai, 1998 and 2003. *Int. J. Biometeorol.* 51, 193–200. <https://doi.org/10.1007/s00484-006-0058-3>.
- Tan, J., Zheng, Y., Tang, X., Guo, C., Li, L., Song, G., Zhen, X., Yuan, D., Kalkstein, A.J., Li, F., Chen, H., 2010. The urban heat island and its impact on heat waves and human health in Shanghai. *Int. J. Biometeorol.* 54, 75–84. <https://doi.org/10.1007/s00484-009-0256-x>.
- Tong, S., Prior, J., McGregor, G., Shi, X., Kinney, P., 2021. Urban heat: an increasing threat to global health. *BMJ* n2467. <https://doi.org/10.1136/bmj.n2467>.
- Weisskopf, M.G., Anderson, H.A., Foldy, S., Hanrahan, L.P., Blair, K., Török, T.J., Rumm, P.D., 2002. Heat wave morbidity and mortality, Milwaukee, Wis, 1999 vs 1995: an improved response? *Am. J. Public Health* 92, 830–833. <https://doi.org/10.2105/AJPH.92.5.830>.
- Xu, Z., Fitzgerald, G., Guo, Y., Jalaludin, B., Tong, S., 2016. Impact of heatwave on mortality under different heatwave definitions: a systematic review and meta-analysis. *Environ. Int.* 89–90, 193–203. <https://doi.org/10.1016/j.envint.2016.02.007>.
- Yang, Jiachuan, Hu, L., Wang, C., 2019a. Population dynamics modify urban residents' exposure to extreme temperatures across the United States. *Sci. Adv.* 5, eaay3452. <https://doi.org/10.1126/sciadv.aay3452>.
- Yang, Jun, Jin, S., Xiao, X., Jin, C., Xia, J., Li, X., Wang, S., 2019b. Local climate zone ventilation and urban land surface temperatures: towards a performance-based and wind-sensitive planning proposal in megacities. *Sustain. Cities Soc.* 47, 101487 <https://doi.org/10.1016/j.scs.2019.101487>.
- Yang, X., Peng, L.L.H., Jiang, Z., Chen, Y., Yao, L., He, Y., Xu, T., 2020a. Impact of urban heat island on energy demand in buildings: local climate zones in Nanjing. *Appl. Energy* 260, 114279. <https://doi.org/10.1016/j.apenergy.2019.114279>.
- Yang, Y., Zheng, Z., Yim, S.Y.L., Roth, M., Ren, G., Gao, Z., Wang, T., Li, Q., Shi, C., Ning, G., Li, Y., 2020b. PM_{2.5} pollution modulates wintertime urban Heat Island intensity in the Beijing–Tianjin–Hebei megalopolis, China. *Geophys. Res. Lett.* 47 <https://doi.org/10.1029/2019GL084288>.
- Yang, Y., Guo, M., Ren, G., Liu, S., Zong, L., Zhang, Yanhao, Zheng, Z., Miao, Y., Zhang, Ying, 2022. Modulation of wintertime canopy urban Heat Island (CUHI) intensity in Beijing by synoptic weather pattern in planetary boundary layer. *JGR-Atmos.* 127 <https://doi.org/10.1029/2021JD035988>.
- Zardi, D., Whiteman, C.D., 2013. Diurnal Mountain wind systems. In: Chow, F.K., De Wekker, S.F.J., Snyder, B.J. (Eds.), *Mountain Weather Research and Forecasting*. Springer Atmospheric Sciences. Springer, Netherlands, Dordrecht, pp. 35–119. https://doi.org/10.1007/978-94-007-4098-3_2.
- Zhang, J., Hou, Y., Li, G., Yan, H., Yang, L., 2005. Satellite remote sensing research and influence factor analysis of diurnal variation and seasonal characteristics of Heat Island in Beijing and its surrounding areas. *Chin. Sci. Earth Sci. Chin.* 187–194.
- Zheng, Z., Ren, G., Gao, H., 2018. Analysis of the local circulation in Beijing area. *Meteorol. Mon. Chin.* 425–433.
- IPCC, 2021. Masson-Delmotte, V., P. Zhai, A. Pirani, S.L. Connors, C. Péan, S. Berger, N. Caud, Y. Chen, L. Goldfarb, M.I. Gomis, M. Huang, K. Leitzell, E. Lonnoy, J.B. R. Matthews, T.K. Maycock, T. Waterfield, O. Yelekçi, R. Yu, and B. Zhou (eds.), 2021. *Climate Change 2021: The Physical Science Basis*. Cambridge University Press. doi:10.1017/97810009157896.

- Zheng, Z., Ren, G., Gao, H., Yang, Y., 2022. Urban ventilation planning and its associated benefits based on numerical experiments: a case study in Beijing, China. *Build. Environ.* 222, 109383 <https://doi.org/10.1016/j.buildenv.2022.109383>.
- Zong, L., Liu, S., Yang, Y., Ren, G., Yu, M., Zhang, Y., Li, Y., 2021. Synergistic influence of local climate zones and wind speeds on the urban Heat Island and heat waves in the megacity of Beijing, China. *Front. Earth Sci.* 9, 673786 <https://doi.org/10.3389/feart.2021.673786>.
- Chen, G., Wang, D., Wang, Q., Li, Y., Wang, X., Hang, J., Gao, P., Ou, C., Wang, K., 2020. Scaled outdoor experimental studies of urban thermal environment in street canyon models with various aspect ratios and thermal storage. *Sci. Total Environ.* 726, 138147. <https://doi.org/10.1016/j.scitotenv.2020.138147>.